SOILS AND FOUNDATIONS Vol. 31, No. 4, 48-60, Dec. 1991
Japanese Society of Soil Mechanics and Foundation Engineering

RELIABILITY ANALYSIS OF REINFORCED EARTH RETAINING STRUCTURES SUBJECTED TO EARTHQUAKE LOADING

D. D. GENSKE[I], T. ADACHI[II] and M. SUGITO[III]

ABSTRACT

In this paper earth retaining walls reinforced with geotextiles are investigated. The failure model considered is a special internal one, where the failure plain cuts through the geotextile layers. Horizontal earthquake forces are introduced to allow a seismic resistant design. Parametric studies indicate that, for the failure model considered, the toe of the reinforced wall is its most sensitive part. Based on the probabilistic safety concept a reliability analysis is carried out and design factors are derived, which permit the assessment of the safety of the structure in an easy and convenient way. More detailed earthquake related studies are carried out in order to compare the design situation between Tokyo, Osaka and Kyoto. It is found that the construction of reinforced earth retaining structures appears to be feasible in Osaka and Kyoto, whereas in Tokyo, because of its prominent earthquake record, especially the toe of the wall has to be designed with great caution in order to ensure the probability of failure to remain acceptably small.

Key words : earthquake resistant, retaining wall, safety factor, stability analysis, statistical analysis (**IGC :** E-6/E-13)

INTRODUCTION

Since the introduction of the reinforced earth method by H. Vidal (1966) it has been proved throughout the world that reinforced walls are often more economical than conventional methods. However, economical design depends very much on the safety factors used for the stability analysis. The question, how large the safety factors should be and whether a global safety factor or partial safety factors should be applied, has not thoroughly been answered yet. This subject becomes even more complicated when dynamic forces such as earthquake loadings are included in the analysis.

A problem of this kind cannot be solved only by empirical evaluation, since we are talking about a fairly new development in geotechnical engineering. In fact, both the mechanical behavior of the geotextile and the failure

I) JSPS Research Fellow, School of Civil Engineering, Kyoto University, Kyoto 606.
II) Professor, School of Civil Engineering, Kyoto University, Kyoto 606.
III) School of Civil Engineering, Kyoto University, Kyoto 606.
Manuscript was received for review on June 27, 1990.
Written discussions on this paper should be submitted before July 1, 1992, to the Japanese Society of Soil Mechanics and Foundation Engineering, Sugayama Bldg. 4 F, Kanda Awaji-cho 2-23, Chiyoda-ku, Tokyo 101, Japan. Upon request the closing date may be extended one month.

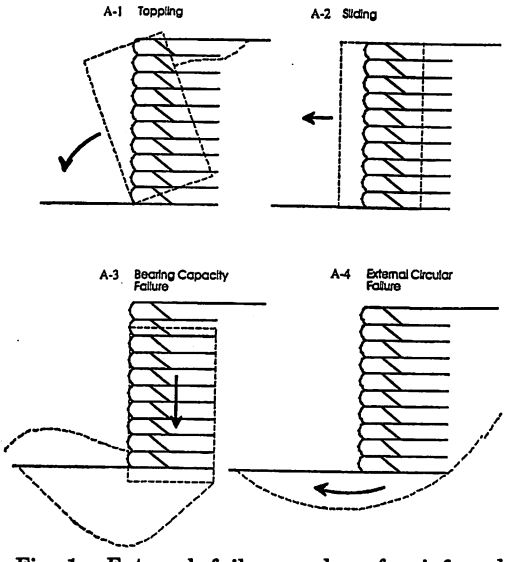

Fig. 1. External failure modes of reinforced earth retaining structures

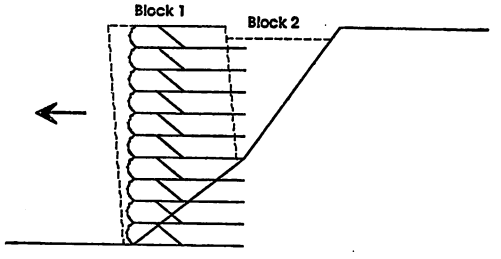

Fig. 2. Global internal failure of a reinforced earth retaining structure (type : B-3)

mechanism are still subjected to research. Thus, the probabilistic approach is one of the effective means to derive safety factors for this type of geotechnical structures.

FAILURE MECHANISMS

An earth retaining structure reinforced by geotextiles can fail due to a variety of failure modes. We have to distinguish between the external and internal failure as in the following.

A. External failure modes
   - A-1 Toppling
   - A-2 Sliding
   - A-3 Bearing capacity failure
   - A-4 External circular failure

B. Internal failure modes
   - B-1 Breaking of the geotextile
   - B-2 Partial pull out of geotextile
   - B-3 Global failure of the structure with a slip surface cutting through the geotextiles

Fig. 1. illustrates the external failure modes. The global internal failure mode is depicted in Fig. 2.

Reinforced earth retaining structures usually also experience considerable settlement. Therefore, special attention should be paid to the settlement potential. But not only the vertical settlement appears to be important. In accordance with Broms (1988) the potential lateral displacement has to be considered as a relevant design criterion. The external failure modes refer to conventional mechanisms, which have been investigated already. The internal failure modes, on the other hand, still require further investigation. This specially concerns failure mode B-3. This study deals with this internal failure mode, B-3, which has not been investigated sufficiently and is considered to be the most critical in a view point of earthquake registant design.

PERFORMANCE FUNCTIONS

Statical Loading Conditions

Recent studies by Gudeshus and Schwing (1986) help to understand this particular type of failure mechanism. Based on laboratory tests a 2-block failure mechanism was identified (Fig. 3) and the following performance function was derived :

$$f(\varphi, \varphi_g, h, l, \vartheta_g)=\sum_{i=1}^{n} Z_i - W\tan(\vartheta_g-\varphi) - E_a\frac{\cos(2\varphi-\vartheta_g)}{\cos(\varphi-\vartheta_g)}\geq 0. \quad (1)$$

with

$$\sum_{i=1}^{n} Z_i = 2\tan\varphi_g \sum_{i=1}^{n}\sigma_i l_i = 2\tan\varphi_g\gamma\sum_{i=1}^{n} h_i l_i$$

$$=2T\gamma\sum_{i=1}^{n} h_i l_i$$

$$W=\frac{1}{2}\gamma h^2(2-b\tan\vartheta_g)b$$

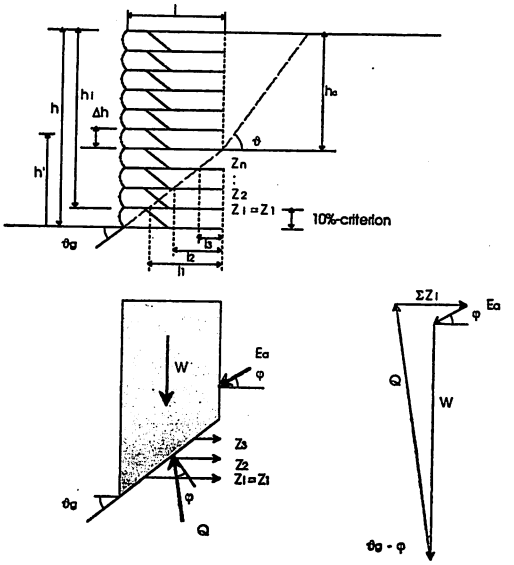

Fig. 3. The 2-block failure mechanism-statical loading conditions

$$E_a=\frac{1}{2}\gamma h_e^2 k_a$$

$$\sigma_i=\gamma h_i$$

$$T=\tan\varphi_g$$

where

φ=angle of internal friction of soil [°]

φ_g=friction angle between geotextile and soil [°]

γ=unit weight of soil [kN/m³]

$b=l/h$ [-]

$k_a=\tan^2(45°-\varphi/2)\sqrt{(1+\sin\varphi)/(1+\sin 3\varphi)}$ [-]

ϑ_g=critical sliding angle of block 1 [°]

n=number of geotextile layers above base layer [-]

$h_e=h(1-b\tan\vartheta_g)$ [m]

For this performance function it was assumed that:

(a) There is no other vertical loading of the wall except that caused by gravity of the soil.

(b) The wall is completely drained.

(c) The earth pressure behind the reinforced wall is calculated in accordance with COULOMBs earth pressure theory.

(d) The slip surfaces of the two blocks meet where the reinforcement ends.

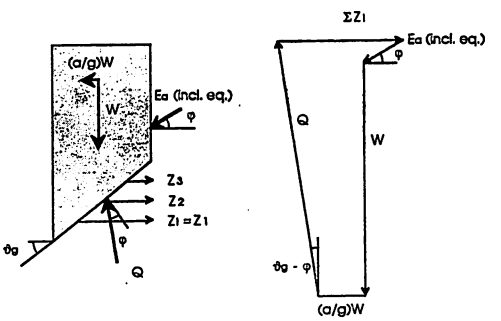

Fig. 4. The 2-block failure mechanism-earthquake loading conditions

(e) The variation of the slip surface of the block 1 yields the minimum of the performance function.

As is shown in the above mentioned article, this 2-block failure mechanism yields the most realistic results. However, as mentioned in the assumptions, a vertical surface loading of the reinforced structure, like storage dead loads or live loads due to vehicular traffic has not been included in this study. Furthermore, lateral horizontal loads resulting from earthquake motions were not considered. This, however, would be essential for reinforced earth structures built in Japan. In this paper, the effect of the horizontal loading on the stability of the 2-block failure system is investigated.

Earthquake Loading

If a reinforced earth retaining structure is subjected to an earthquake loading, the two blocks of the global internal failure model will be subjected to an earthquake acceleration. Horizontal earthquake accelerations directed towards the open side of the retaining wall will destabilize the system considerably. The horizontal accelerations cause horizontal forces as depicted in Fig. 4. They are a function of the mass of each block and the horizontal acceleration due to the earthquake. In order to derive a performance function for the system, the following assumptions were made:

(a) No additional vertical loading of the wall itself and the area behind the wall is considered.

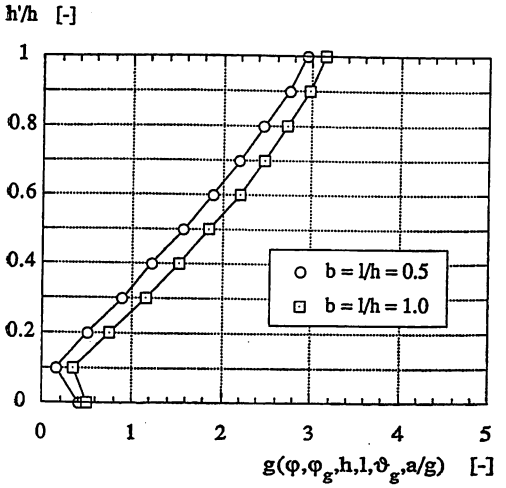

Fig. 5. The dimensionfree results of the performance function (Eq. (2)) over the normalized height of the reinforced earth structure. Variation of the geometry factor $b=l/h$. $\varphi=\varphi_g=30°$, $\Delta h/h=0.1$, $\tilde{a}=0$

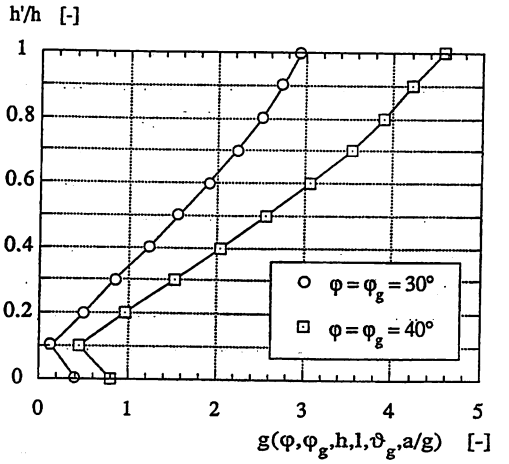

Fig. 6. The dimensionfree results of the performance function (Eq. (2)) over the normalized height of the reinforced earth structure. Variation of the angle of internal friction $b=0.5$, $\Delta h/h=0.1$, $\tilde{a}=0$

(b) Only horizontal earthquake accelerations were applied.

(c) No liquefaction effect or related phenomena were taken into account.

(d) Due to the settlement of the wall, a pre-existing sliding surface for block 2 is assumed. Its inclination was calculated from COULOMBs earth pressure theory.

Concerning the last assumption it will be shown, however, by the end of this article that the safety factors derived in the following reliability analysis can also be applied to the case of an earthquake induced sliding plane as described by Mononobe-Okabe's formula (1984).

Based on these assumptions, which represent a simplified statical approach, the following performance function was derived (Adachi and Genske, 1990):

$$g(\varphi,\ \varphi_g,\ h,\ l,\ \vartheta_g,\ \tilde{a})$$
$$=2\tan\varphi_g\sum_{i=1}^{n}\frac{h_i l_i}{h\cdot l}$$
$$-\frac{1}{2}(2-b\tan\vartheta_g)\{\tan(\vartheta_g-\varphi)+\tilde{a}\}$$
$$-\frac{1}{2}\frac{1}{b}(1-b\tan\vartheta_g)^2\{1+\tilde{a}\cot(\vartheta-\varphi)\}\kappa\geq 0. \qquad (2)$$

with, besides the parameters mentioned already in Eq. (1):

$\tilde{a}=a/g$=horizontal earthquake acceleration over g [-]

$$\vartheta=\operatorname{atan}(\tan\varphi+\sqrt{0.5}/\cos\varphi)$$

$$\kappa=\cot\vartheta\ \frac{\sin(\vartheta-\varphi)}{\cos(\vartheta-2\varphi)}\ \frac{\cos(2\varphi-\vartheta_g)}{\cos(\varphi-\vartheta_g)}$$

Fig. 5 gives the dimension-free results of this performance function $g(\varphi,\ \varphi_g,\ h,\ l,\ \vartheta_g,\ \tilde{a})$ over the normalized height h'/h (see Fig. 3) of the reinforced earth structure. The larger this value is, the safer is the structure. If $g(\varphi,\ \varphi_g,\ h,\ l,\ \vartheta_g,\ \tilde{a})$ drops below zero, the structure fails. Two different geometries are considered: $b=l/h=1$ refers to a length of reinforcement as long as the height of the wall, whereas $b=0.5$ represents a reinforcement length half as large as the height. Two results are obvious:

(a) With decreasing b the stability, as expected, decreases as well.

(b) In the vicinity of the toe of the wall the safety of the structure has a minimum.

The second finding leads to the important conclusion, that for the failure mode considered, the toe of the wall is the most sensitive

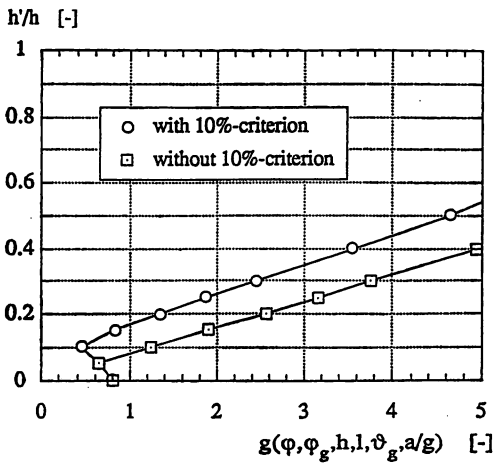

Fig. 7. The 10%-Criterion
$\varphi=\varphi_0=40°$, $\Delta h/h=0.05$, $b=0.5$, $\tilde{a}=0$

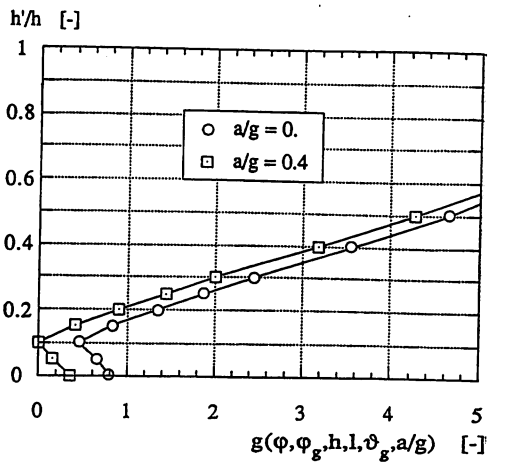

Fig. 8. Increase of the earthquake acceleration
$\varphi=\varphi_0=40°$, $\Delta h/h=0.05$, $b=0.5$,
10%-Criterion included

part and special caution has to be taken in order to ensure the proper design of this area.

In a second parametric study (Fig. 6), the internal friction angle was increased from 30° to 40°. The effect on the safety of the structure is quite clear. As expected, the safety increases with increasing internal friction angle.

Gudehus and Schwing (1986) state in their paper, that, based on field tests of Gudehus and Gassler (1981), the geotextiles of the lower 10% of the wall do not contribute to the overall stability. Therefore, the geotextiles in this portion of the wall have to be ignored. In connection with the conclusion drawn above, that the toe is the most sensitive part of the wall, this statement is very important, indeed. Fig. 7 juxtaposes the performance of the structure with and without consideration of this 10%-criterion. The stability decreases considerably, if the 10%-criterion is included. To be on the safe side, the following parametric studies all consider the 10%-criterion.

The last deterministic parametric study (Fig. 8) shows, how the stability of the structure decreases, if an earthquake occurs and with it a horizontal acceleration. This decrease of stability is especially drastic in the vicinity of the toe of the wall.

In the next section, the probabilistic performance of the reinforced wall will be discussed.

RELIABILITY ANALYSIS

State of Art

During the last two decades, the probabilisic approach has become a most valuable tool in solving engineering problems. In fact, only the probabilistic approach can give us a quantitative assessment of the safety of a structure, provided we know its performance function and the statistics of the parameters involved. The probabilistic approach not only helps us to assess the safety of a structure in terms of the probability of failure, it also allows us to derive probability based safety factors. These safety factors can be derived for a given tolerable probability of failure.

Among the possible procedures to derive the failure probability and appropriate safety factors, the Invariant Second Moment Approach by Hasofer and Lind (1974) has proven to be very effective and easy to understand. A good explanation of this method is given in Ang and Tang (1984).

In the paper of Gudehus and Schwing (1986) mentioned above, this method was applied in order to calculate partial safety factors. They were derived for the internal friction and the friction angle between the fabric and the soil, since these two parameters show a considerable dispersion. All other parameters of the

performance function were considered to be deterministic (not dispersive) or to have a negligible dispersion.

As for the 2-block failure mechanism, there are two aspects which still need closer investigation :

1. The analysis of a vertically loaded reinforced earth structures. Of interest here is especially the live load, since it would have a statistical distribution which might be difficult to model.
2. The stochastic interpretation of earthquake loadings and their effect on the reinforced earth structure.

This paper is concerned with the second aspect. In order to perform a reliability analysis of retaining walls subjected to earthquake loadings, stochastic models have to be derived for the parameters of the performance function (Eq. (2)). After the stochastic models have been established, a probabilistic analysis can be carried out. Finally, partial safety factors for the dispersive parameters, also called design factors, can be derived.

Derivation of the Stochastic Models

Of all parameters of the performance function for earthquake loaded reinforced retaining walls (Eq. (2)) three have to be considered as dispersive : The angle of internal friction of the sand, the friction coefficient between the fabric and the sand and the earthquake acceleration. Although other parameters like the unit weight or the geometry of the wall may also have some dispersion, their standard deviations are rather small compared with the 3 dispersive parameters mentioned before and are therefore neglected.

In accordance with Gudehus and Schwing (1986) the friction coefficient T between the fabric and the soil is interpreted as GAUSS-normal distributed with a coefficient of variation (COV) ranging from

$$0.10 \leq COV_T \leq 0.15, \quad T = \tan \varphi$$

The internal friction angle is considered to be lognormally distributed. Its COV may range, in accordance with Gudehus and Schwing (1986) and Genske and Walz (1987) between the following boundaries :

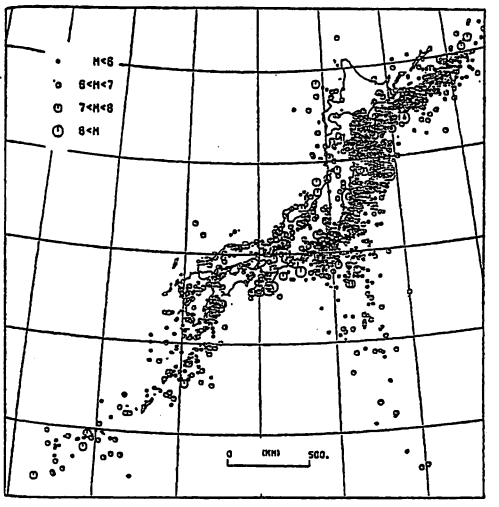

Fig. 9. Distribution of disastrous earthquakes in Japan from historical records (Usami 1975)

$$0.05 \leq COV_\varphi \leq 0.10$$

For simplicity, the probability density function is considered to be bound at zero to the left hand side.

The stochastic model for the seismic load is much more complicated. The statistics of the frequency and the magnitude of earthquakes depends strongly on the area considered. Fig. 9 illustrates the regional distribution of disastrous earthquakes which occurred in Japan during the last 800 years (Usami 1975). The map shown is based on historical occurrence data. Especially along the Pacific Ocean Coast, where the Pacific Plate subduces under the Japan Island, the frequency of earthquakes is rather high.

Based on these data, the annual probability of occurrence can be derived for every region in Japan. As shown in Fig. 10 the annual probability of occurrence U(M, Δ) for Tokyo, Osaka and Kyoto is given. U(M, Δ) is a function of the magnitude M and the distance Δ of the epicenter to the region considered. These characteristic local earthquake probabilities allow the derivation of earthquake hazard curves. With the attenuation equation for the horizontal peak acceleration (Sugito, 1986)

$$\bar{a} = f(\mathrm{M}, \Delta) = \begin{cases} 111 \times 10^{0.534\mathrm{M}}/(\Delta+30)^{1.857} ; & \Delta \geq \Delta_0(\mathrm{M}) \\ 99.6 \times 10^{0.0846\mathrm{M}} ; & \Delta < \Delta_0(\mathrm{M}) \end{cases} \quad (3)$$

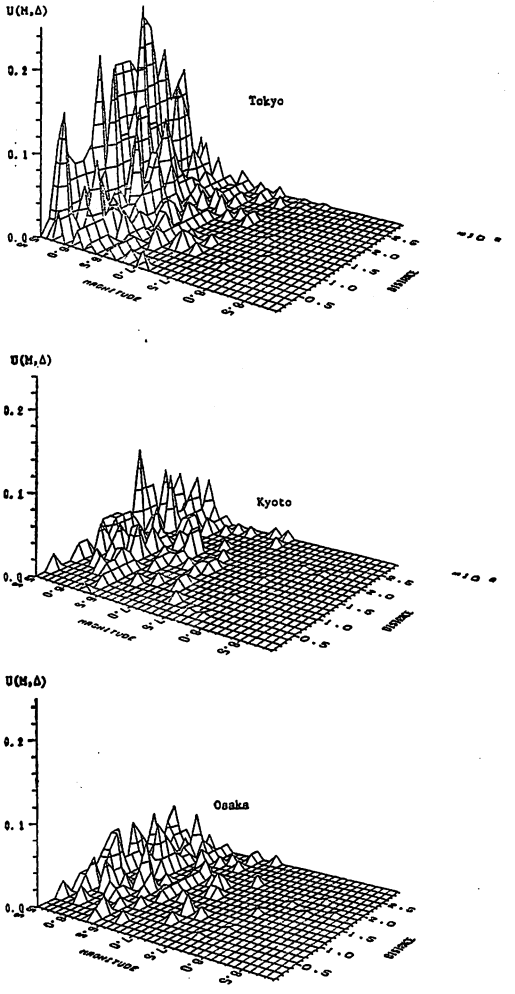

Fig. 10. Annual probability of occurrence U (M, Δ) as a function of the magnitude M and the distance from the epicenter Δ for Tokyo, Kyoto and Osaka

$\bar{a}$=estimated peak acceleration [cm/s^2]
M=Magnitude on the RICHTER-Scale [-]
Δ=distance of location considered to epicenter [km]
$\Delta_0=\Delta_0(M)=1.06\cdot10^{0.242M}-30$; $(M \geq 6.0)$ [km]
the annual probability of exceedance for a given peak acceleration a can be calculated:

$$P(a)=\sum_{M_i}\sum_{\Delta_j} P(\bar{a}>a \mid M_i, \Delta_j)U(M_i, \Delta_j) \quad (4)$$

in which $P(\bar{a} > a \mid M_i, \Delta_j)$ represents the probability that the peak acceleration $\bar{a}$ exceeds a for given magnitude M_i and distance Δ_j. The

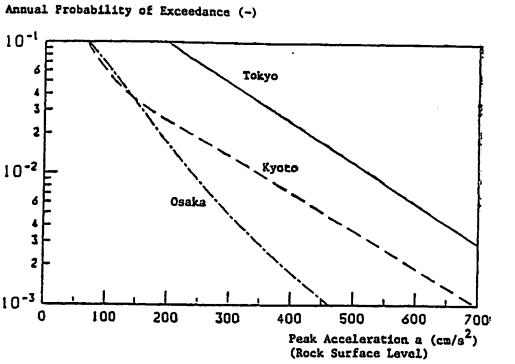

Fig. 11. Earthquake hazard curves for Tokyo, Osaka and Kyoto

Table 1. Normalized peak acceleration for given annual exceedance probability

Annual Exceedance Probability [-]	Osaka $\bar{a}=a/g$	Kyoto $\bar{a}=a/g$	Tokyo $\bar{a}=a/g$
1/10	0.07	0.07	0.20
1/50	0.18	0.23	0.43
1/100	0.24	0.35	0.53

lognormal distribution is assumed for the estimation of peak acceleration.

Plotting $P(a)$ over the peak acceleration gives the hazard curves for the Tokyo, Osaka and Kyoto (Fig. 11). By means of these hazard curves, peak accelerations for given time intervals, also called return periods, can be estimated. For the design purpose, the live time of the structure will specify the return period. Table 1 gives the normalized peak accelerations $\bar{a}=a/g$(a=peak acceleration, g= gravitational acceleration) for three values of annual exceedance probability for Osaka, Kyoto, and Tokyo.

The peak accelerations derived, however, refer to hard ground conditions. In order to modify the peak accelerations for local ground conditions, a conversion factor B has to be taken into consideration (Sugito and Kameda 1990) :

$$a_L=B\cdot a \quad (5)$$

a_L=peak acceleration for local ground condition [cm/s^2]
a=peak acceleration for hard ground condi-

tion [cm/s²]

B=conversion factor [-]

The conversion factor is a function of the blow count number related to the soil of the site under investigation, the depth to the bedrock and the peak acceleration a. It includes the nonlinear amplification effects of the local soil layers on the ground motion.

Because the final peak acceleration depends on a variety of dispersive input data, it also has to be regarded as dispersive. However, the grade of dispersion is not easy to assess and depends on the location considered. For this study, only the mean values were considered.

Finally it should be mentioned, that in this approach only the peak acceleration was considered. For further studies on this topic it is recommended to also include the effect of the duration of the ground motion and the spectral intensity. Since hazard curves which include these effects can also be derived their consideration should be possible.

Probabilistic Interpretation

In order to ensure the safety of a structure, appropriate safety factors are needed. On the basis of the probabilistic safety concept partial safety factors can be derived. These partial safety factors are applied directly to the parameters which have been recognized as statistically dispersive ones.

The mean value of the peak acceleration, which is used to calculate the horizontal earthquake loads, depends on the annual probability of exceedance. This annual probability of exceedance defines the return period and is therefore used to specify the live time of the structure. In this paper the earthquake statistics only assists in deriving the design earthquake loads. Since these design loads already include a statistical model, they are interpreted as deterministic (i. e. not dispersive) in the subsequent reliability analysis. Although this procedure includes some approximations, it has the advantage of being easy to apply and flexible as to the local characteristics of the earthquake record.

Thus, only the internal friction angle and the friction coefficient are considered to be dispersive for the derivation of their design factors. Probabilistic design factors ensure a certain probability of failure not to be exceeded. In accordance with First Order Second Moment Approach (Hasofer and Lind 1974) the design factor for the GAUSS-normal distributed friction coefficient T is determined by

$$\gamma_T = \frac{\mu_T}{T^*} \tag{6}$$

whereas for the lognormal distributed internal friction angle it follows that

$$\gamma_\varphi = \frac{\hat{\mu}_\varphi^N}{\hat{\varphi}^*} \tag{7}$$

where

γ_T, γ_φ=design factors for T and φ [-]

μ_T=mean value of T [-]

$\hat{\mu}_\varphi^N$=mean value of the lognormal $\hat{\varphi}$, transformed to its GAUSS-normal equivalent [-]

$=\hat{\varphi}^*(1-\ln\hat{\varphi}^*-\lambda)$

T^*=design point of $T=\mu_T-\alpha_T\beta\sigma_T$ [-]

$\hat{\varphi}^*$=design point of $\hat{\varphi}=\hat{\mu}_\varphi^N-\alpha_\varphi\beta\hat{\sigma}_\varphi^N$ [-]

β=safety index [-], from

$p_f=\Phi(-\beta)$=probability of failure [-], where

$\Phi()$=Cumulative GAUSS-normal probability function [-]

σ_T=standard deviation of T [-]

$\hat{\sigma}_\varphi^N$=to its GAUSS-normal equivalent transformed standard deviation of the lognormal $\hat{\varphi}$ [-]

$=\hat{\varphi}^*\zeta$

$$\lambda=\ln\hat{\mu}_\varphi-\frac{1}{2}\zeta^2 \text{ [-]}$$

$$\zeta=\sqrt{\ln(1+\sigma_\varphi^2/\mu_\varphi^2)}\cong COV_\varphi \text{ [-]}$$

$$\alpha_T=\frac{\left(\frac{\partial g}{\partial T'}\right)_*}{\sqrt{\left(\frac{\partial g}{\partial \varphi'}\right)_*^2+\left(\frac{\partial g}{\partial T'}\right)_*^2}}$$

$$\alpha_\varphi=\frac{\left(\frac{\partial g}{\partial \varphi'}\right)_*}{\sqrt{\left(\frac{\partial g}{\partial \varphi'}\right)_*^2+\left(\frac{\partial g}{\partial T'}\right)_*^2}}$$

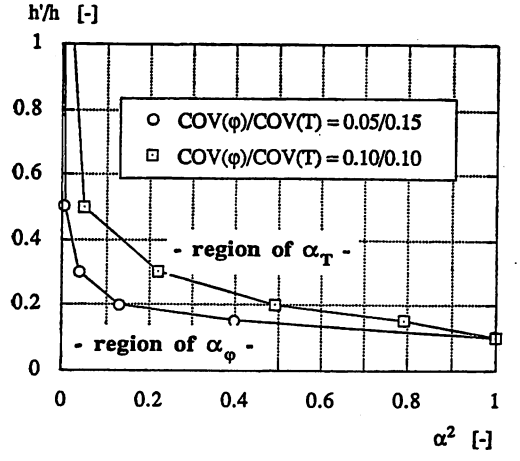

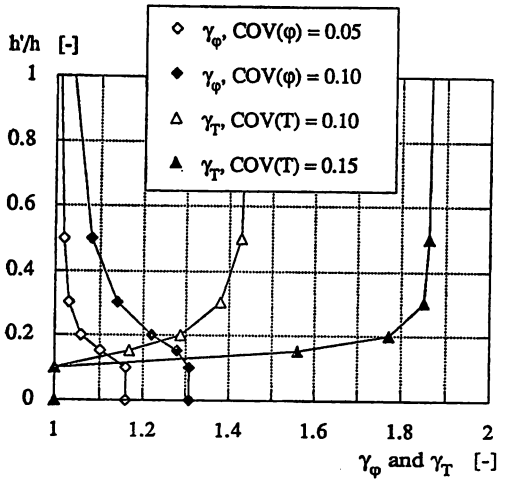

Fig. 12. α^2-values as a function of the normalized height of the wall h'/h and the resulting safety factors γ_φ and γ_T. Constant failure probability maintained at 1/1000 $\mu_\varphi=40°$, $\mu_T=0.839=\tan(40°)$, $b=0.5$, $\Delta h/h=0.05$, 10%-Criterion satisfied

$$\frac{\partial g}{\partial T'} = \sigma_T \frac{\partial g}{\partial T}$$

$$\frac{\partial g}{\partial \hat{\varphi}'} = \partial_\varphi^N \frac{\partial g}{\partial \hat{\varphi}}$$

These relationships show, that in order to calculate the partial safety factors the values of α have to be determined, which are functions of the partial derivatives of the performance function to the dispersive parameters.

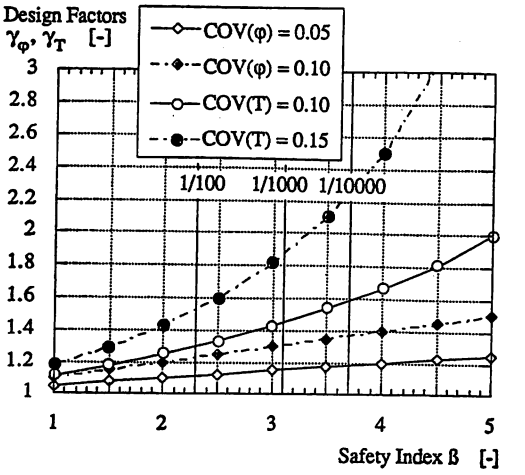

Fig. 13. Conservative design factors for φ and T with increasing failure probability

The results can only be found by means of an iterative procedure. From the definition of the α-values it follows that

$$\alpha_\varphi^2+\alpha_T^2=1.0 \qquad (8)$$

This means, that with increasing α the relative effect of the dispersive parameter associated with this α on the failure probability will also increase, and so will the partial safety factor. In Fig. 12 the α^2-values and the safety factors associated with these α's are plotted over the height of the reinforced wall. The failure probability in this study was fixed to 1/1000, which refers to a safety index of $\beta=3.1$.

In the lowest part of the wall, where the geotextiles do not contribute to the safety of the 2-block system, the α for the internal friction angle is 1.0, since φ is the only dispersive parameter contributing to the safety of the structure. Consequently, the partial safety factor has a constant value. As soon as the geotextile starts supporting the system, an α for the friction coefficient T generates. The increase of α_T will be especially large, if the COV of the friction coefficient T is also large relative to φ. The region, where both dispersive parameters have a considerable effect on the safety of the wall is rather limited, however. The α_T will, with increasing heights

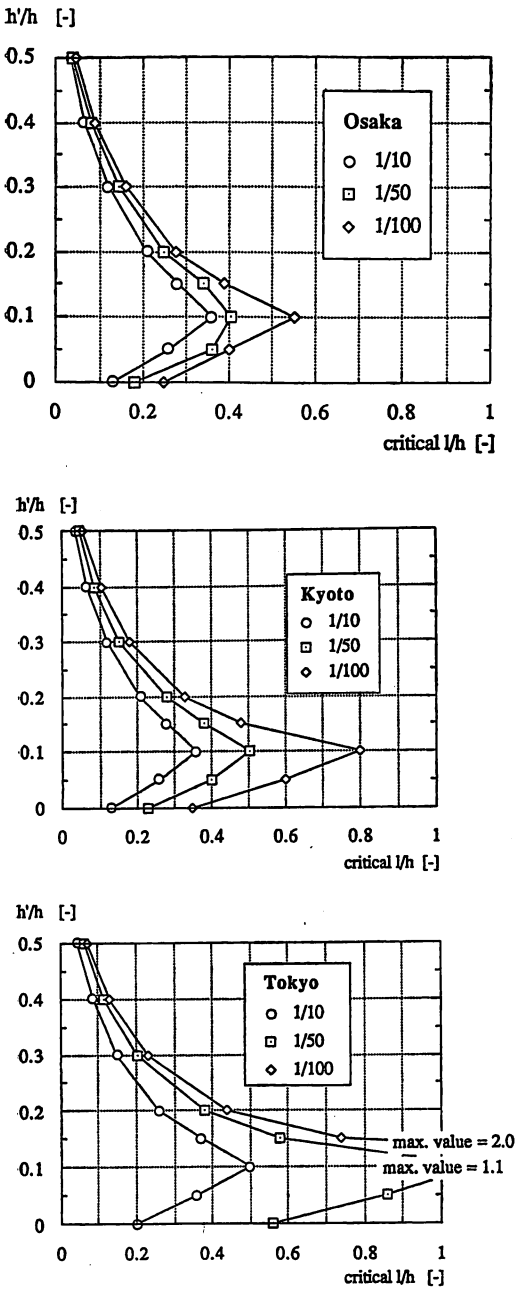

Fig. 14. The critical geometry $b=l/h$ plotted over the normalized height of the wall h'/h for Osaka, Kyoto and Tokyo. Three annual exceedance probabilities (1/10, 1/50, 1/100) of the local earthquake peak acceleration as illustrated in Fig. 11 are considered. The design factors for the friction parameters φ (internal friction) and T (geotextile) refer to a tolerable failure probability of 1/1000. The 10%-Criterion is satisfied
$\mu_\varphi=\mu_T=40°$, $COV_\varphi=0.075$, $COV_T=0.125$, $\gamma_\varphi=1.2$, $\gamma_T=1.7$

h'/h, soon dominate the failure probability, even if its COV is at the lowest possible limit.

If Fig. 12 is now compared with the plots discussed above, where the values of the performance function are represented in the same manner, we have to realize, that the region of uncertain α's refers to the most sensitive part of the wall, where the deterministic safety already has a minimum. Therefore, no attempt has been made to monitor the behavior of the α's with further parametric studies. It is rather suggested to approximate both α's with their possible upper value, which is 1.0. With this assumption we achieve to be on the safe side as to this critical part of the wall.

Utilizing the relationships pointed out in Eq. (6) through (8), the partial safety factors necessary to ensure a certain probability of failure (expressed by β) not to be exceeded are given by

$$\gamma_T=\frac{1}{1-\alpha_T\beta_{covT}} \qquad (9)$$

$$\gamma_\varphi=\frac{1}{\left(1-\frac{\alpha_\varphi\beta\zeta}{1+\alpha_\varphi\beta\zeta}\right)} \qquad (10)$$

Fig. 13 gives the partial safety factors calculated as a function of the safety index β. With increasing β, which refers to a decrease in the tolerable failure probability, the safety factors increase as well. The upper and lower margins of the COV of both parameters are given. For a large COV, the required safety factor must be large, too. Also indicated are the recommended failure probabilities for geotechnical structures (Meyerhof, 1982). If the failure of the wall has only a minor economical impact, the lower boundary is appropriate, whereas if losses of lives have to be expected in case of a failure, the upper limit is recommended.

It may be mentioned, that these safety factors can also be applied, if an earthquake in-

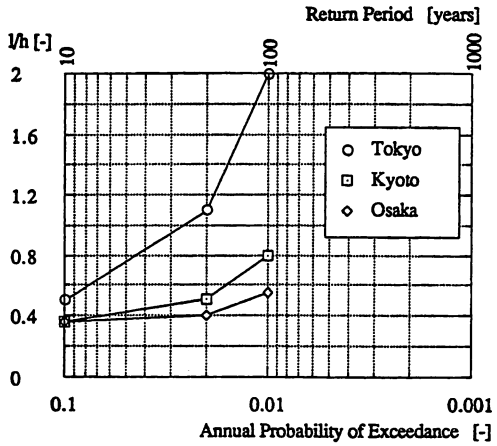

Fig. 15. The critical geometry $b=l/h$ as a function of the annual exceedance probability. Input data are the same as in Fig. 14

duced failure plane for the earth pressure on block 2 is assumed (see *Earthquake Loading*, last assumption). This is due to the fact, that in this case the distribution of α-values over the height of the wall looks similar and consequently the same conclusions as to the approximation of the safety factors are allowed.

Fig. 14 gives the allowable geometry $b=l/h$ of a reinforced wall for the locations Osaka, Tokyo and Kyoto as a function of the height h of the wall, normalized with the height h' of the point of calculation (use Fig. 3 to recall the geometry). The mean internal friction angle μ_φ and the mean friction coefficient μ_T of the geotextile are reduced by the appropriate safety factors γ_φ and γ_T from Fig. 13 to ensure a failure probability of 1/1000. The input data are specified in the figure. In this parametric study the earthquake return period was varied from 10 to 100 years as suggested in *Deviation of Stochastic Models* of this paper. It follows from this evaluation that

(a) as expected, with increasing length of the return period the critical geometry ratio increases as well,
(b) the foot of the wall again proves to be the most sensible part of the reinforced structure,
(c) for the Osaka region much smaller geometry ratios $b=l/h$ are allowed in comparison with Tokyo, whereas Kyoto has an intermediate position.

Fig. 15 likewise illustrates these results. Here the critical geotextile length l (normalized with the wall heights h) in the toe zone is plotted over the earthquake return period. Whereas for Osaka and Kyoto long return periods still yield feasible reinforcement length, a geotextile structure in Tokyo allows, from the practical point of view, only rather short return periods.

It is clear from these graphs that the construction of reinforced earth walls is practicable without problems in the Osaka and Kyoto areas, whereas in the Tokyo region the required length of reinforcement at the toe of the wall may limit the application of this type of earth retaining structures. In those cases, the length of the geotextiles in the toe section can be reduced by using a sand with a rather high internal friction angle. Furthermore, the *COV* of the sand should be minimized, thus allowing more economical safety factors as pointed out in Fig. 13. If still these measures are not sufficient to reduce the length of the geotextiles, the design of the toe of the wall has to be modified.

This study indicates that 4 parameters control the required reinforcement length:

- the internal friction angle and its *COV*
- the local peak earthquake acceleration and its return period.

The friction angle between the geotextile and the soil, as well as its *COV*, are of minor importance for this particular failure model. This is because of the 10%-criterion described in *Earthquake Loading*, which indicates, that in most cases the friction coefficient of the geotextile has none or only little effect at the toe of the wall, which, however, is the most sensitive part of the reinforced structure.

It should be kept in mind, that these findings apply only to the two-block internal failure mechanism discussed above.

SUMMARY

The major conclusions derived from this

study may be summarized as follows.

(1) A reinforced earth retaining structure can fail because of a variety of failure modes. In this paper, an internal failure mode is investigated, which assumes a two-block failure mechanism. The first block (block number 1) is reinforced by geotextiles. This lower sliding plane may cut through the geotextiles, thus causing local pullout failures of geotextiles affected. The stability of the system is decreased if horizontal earthquake forces are introduced. This type of loading condition, however, has to be taken into consideration for every structure built in Japan. Therefore, a performance function was derived for the internal failure mode of the earthquake loaded earth retaining wall.

(2) In order to establish design criteria for this type of failure mechanism, a reliability analysis was carried out, during which design factors were derived. Parametric studies indicated, that the internal friction angle and the friction coefficient between the geotextile and the soil are appropriate for the application of design factors. These design factors are a function of the probability of failure considered to be tolerable. For the earthquake induced horizontal forces the derivation of design loads is treated separately, since the earthquake loading is in contrast to all other parameters a time depended parameter.

(3) During this reliability analysis it was found that the most sensitive part of the reinforced wall is the vicinities of its toe. In the lower 10~20% of the wall the geotextile reinforcement has to be relatively long. Therefore, it was concluded that especially this part of the wall has to be investigated and treated with caution. Furthermore, from the regional analysis of the earthquake peak accelerations it was learned that, given a constant tolerable failure probability and a constant return period for the earthquake, the design situation is most unfavorable in Tokyo, whereas in Kyoto and Osaka design problems as to this failure mode are relatively not critical.

Further research should be directed towards the reliability analysis for other failure modes of the reinforced wall, the consideration of a lateral vertical loading of the upper part of the wall and a more detailed analysis of the dispersive character of the local peak acceleration and its influence on the reliability of the structure.

ACKNOWLEDGMENT

This project has benefited considerably from the basic investigations and laboratory tests on statically loaded reinforced walls, carried out by Professor Dr. Gudehus and Dr. Schwing at the University of Karlsruhe, West Germany. We are also very grateful for the financial support which was granted to us from the Japanese Society for the Promotion of Science (JSPS), Tokyo.

NOTATION

a : peak acceleration [cm/s^2]
$\tilde{a}$: horizontal earthquake acceleration over g [-]
B : seismic conversion factor [-]
b : $=l/h$ [-]
COV : coefficient of variation [-]
h : height of the wall [m]
l : length of reinforced part of the wall [m]
M : magnitude on the RICHTER-Scale [-]
n : number of geotextile layers above base layer [-]
T : $=\tan\varphi_g$ [-]
α_φ, α_T : direction cosines (from probability theory) [-]
β : safety index [-]
γ : unit weight of sand [kN/m^3]
γ_φ, γ_T : design factors for φ and T [-]
Δ : distance to epicenter [km]
ζ : parameter of the lognormal distribution [-]
ϑ : critical angle of active earth pressure [°]
ϑ_g : critical sliding angle of block 1 [°]
λ : parameter of the lognormal distribution [-]
μ_φ, μ_T : mean values of φ and T [°], [-]
σ_φ, σ_T : standard deviations of φ and T [°], [-]
φ : internal friction angle [°]
φ_g : critical sliding angle of block 1 [°]

REFERENCES

1) Ang, A. H. S. and W. H. Tang (1984) : Probability Concepts in Engineering Planing and Design, -Vol. 2.- Wiley & Sons, New York.

2) Broms, B. B. (1988) : "Fabric reinforced retaining walls," Int. Geotechnical Symposium on Theory an Practice of Earth Reinforcement, Fukuoka.
3) Genske, D. D. and B. Walz (1987) : "Anwendung der probabilistischen Sicherheitstheorie auf Grundbruchberechnungen," Géotechnik 10, Vol. 2, pp. 53-66.
4) Gudehus, G. and E. Schwings (1986) : "Standsicherheit kunstoffbewehrter Erdbauwerke an Geländesprüngen," Baugrundtagung Nürnberg FRG, pg. 129-147.
5) Gudehus, G. and Gassler, G. (1981) : "Soil-nailing-Some aspects of a new technique," ICSMFEX, Proc. Vol. 3, Sess 12, pp. 665-670, Stockholm.
6) Hadofer, A. M. and N. C. Lind (1974) : "Exact and invariant second moment code format," J. Engineering Mechanics, Vol. 100, No EM1.
7) JSCE (Japan Society of Civil Engineers) (1984) : "Earthquake Resistant Design for Civil Engineering Structures in Japan."
8) Meyerhof, G. G. (1982) : Limit state design in geotechnical engineering," Structural Safety, 1, pp. 67-71.
9) Sugito, M. (1986): "Earthquake motion prediction, microzonation and burried pipe response for urban seismic damage assessment," School of Civil Engineering, Kyoto University.
10) Sugito, M. and H. Kameda (1990): "Nonlinear soil amplification model with verification by vertical strong motion array records," 4th National Conference on Earthquake Engineering, Palm Springs, USA.
11) Usami, T. (1975): "Descriptive Catalog of Disaster Earthquakes in Japan (in Japanese)," University of Tokyo Press, Tokyo.
12) Vidal, H. (1966): "La Terre Armee.-Annales de l'Institut Technique de Batiment et des Travaux Publics, Nos. 223-229, Paris, pp. 888-939.